Supplemental Material

Detailed Methods

Experimental animals

Mice with inducible endothelial cell-specific p53 deletion (End.p53-KO) were generated and the significant reduction of p53 expression in primary endothelial cells confirmed, as described.[1] In brief, mice with loxP-flanked (floxed, fl) p53 alleles (C57BL/6 background)[2] were mated with mice transgenic for Cre recombinase expressed under control of the Tie2 promoter fused to a mutated murine estrogen receptor ligand-binding domain (C57BL/6 background).[3] Cre recombinase activity was induced with tamoxifen-containing rodent chow (TD55125; Harlan Teklad).[3] The endothelial cell specificity of the inducible Tie2 promoter has been demonstrated previously.[3-5] Cre-WT x $p53^{fl/fl}$ mice fed tamoxifen were used as controls (End.p53-WT). In preliminary analyses, Cre-WT x $p53^{fl/fl}$ mice fed normal rodent chow were also examined (tamoxifen control) and found not to differ with respect to venous thrombosis (data not shown). Age- and sex-matched littermates were used throughout the study. All animal care and experimental procedures had been approved by the institutional Animal Research Committee and the State Office for Consumer Protection and Food Safety and complied with national guidelines for the care and use of laboratory animals.

Mouse model of venous thrombosis

Venous thrombosis in mice was induced by subtotal IVC ligation according to [6-8] with minor modifications. The model of subtotal ligation was chosen to allow the detection of pro- as well as anti-thrombotic effects. Only male mice were examined to minimize any sex-specific influences on the susceptibility to venous thrombosis. Mice were anesthetized by intraperitoneal injection of a mixture of midazolam (5.0 mg/kg body weight [BW]),

medetomidine (0.5 mg/kg BW) and fentanyl (0.05 mg/kg BW). A midline laparotomy incision was made and the IVC was atraumatically exposed immediately below the renal veins. A 5-0 Prolene suture (Ethicon) was placed alongside the IVC as a spaceholder. A stenosis was produced by tying a 6-0 silk suture (Resorba) around the IVC. Subsequently, the spaceholder was removed to allow blood to pass the vessel occlusion. Side or back branches were not ligated. The intestines were relocalized, and the abdominal wall was sutured using 6-0 Ethilon suture (Ethicon). At the end of the procedure, sedation was reversed with atipamezole (0.05 mg/kg BW) and flumazenile (0.01 mg/kg BW). As analgesic, buprenorphine hydrochloride was subcutaneously injected at day 1 and day 2 post-surgery (0.075 mg/kg BW). In some experiments, 12 or 52 week-old male C57BL/6J mice (JANVIER laboratories) were subcutaneously injected with tissue factor pathway inhibitor-2 (TFPI2) peptides (2 mg/g BW in sterile phosphate-buffered saline [PBS]) or PBS alone 30 min before and every 24 hours after subtotal IVC ligation, according to previously described protocols.[9] Two days later, IVC segments (including thrombus and vein wall) were removed and weighed.

High frequency ultrasound measurements

On day 1, 7, 14 and 21 after surgery, mice were anesthetized via inhalation of 2.5% isoflurane (mixed with 0.2 liters per minute [L/min] 100% O_2), and anesthesia was maintained with a face mask (0.5-1.5% isoflurane with 0.05-0.1 L/min 100% O_2). Animals were kept on a heated table mounted on a rail system (VisualSonics). Heart rate was monitored and kept at 500 beats per minute. The extent of venous thrombosis was determined using high frequency ultrasound (Vevo770 system) and a 40 MHz mouse scanhead (Visual Sonics). All measurements were performed by trained medical personnel blinded to the strain and the experimental conditions. The abdomen of the mouse was depilated, and warm ultrasound transmission gel was applied to enable visualization and optimize image quality. First, a long

axis view was taken using the pulse-wave (PW) Doppler mode to visualize the blood flow in the aorta, followed by focussing on the IVC, ligation site and/or thrombus. An optimal freeze-frame image was obtained (based on the careful assessment of *real-time* video sequences) and the longitudinal cross-sectional area of the clot was traced using the Vevo 770 software. Thrombus length and width were measured in triplicate in each mouse on the site of maximum cross-sectional extension of the thrombus applying B-mode and the cross-sectional area calculated ('thrombus size').

Histology and immunohistochemistry

Two days or three weeks following surgery, mice were anesthetized using 2.5% isoflurane. The venous tissue starting immediately distal of the ligature until the iliac bifurcation (approximately 1 cm) was removed together with its surrounding tissue and fixed in 4% zinc formalin. Serial 5 µm-thick paraffin-embedded cross sections, equally spaced through the thrombosed vein segment were cut and stained with Masson Trichrome (MTC) to visualize fibrinogen (red signal), fibrosis (blue signal) and cell nuclei (black signal). Image analysis software (Image Pro Plus; Media Cybernetics) was used to quantify the amount of red/unresolved material (count-size function) and the thrombus cross-sectional area (measure function). Per mouse, 3 sections (approximately 300 µm apart) were evaluated and the results averaged. Carstairs stain was employed to visualize platelets (gray-blue) and erythrocytes (yellow). A schematic representation of the cutting scheme is given in Supplemental Figure S1.

Immunohistochemistry was performed using monoclonal rat anti-mouse Mac2 antibodies (clone M3/38; Biozol) to visualize macrophages, rabbit anti-mouse CD3 antibodies (clone SP7; abcam) to detect lymphocytes, ~~and~~ rat anti-mouse CD31 antibodies (clone Mec13.3; Santa Cruz Biotechnology) to stain endothelial cells, rat anti-mouse CD41 antibodies (clone MWReg30; EXBIO) to visualize platelets and rat anti-mouse ELANE

antibody (clone NIMP-R14; abcam) to detect neutrophils. Following incubation with anti-rat or anti-rabbit secondary antibodies (Molecular Probes), avidin-biotin complexes (ABC-Link; VectorLabs) and peroxidase substrate (aminoethylcarbazole; VectorLabs) were applied. Sections were counterstained with Gill's hematoxyline (Sigma), mounted in ImmuMount (ThermoScientific) and inspected at an Olympus BX51 microscope. All morphometric analyses were performed using image analysis software (Image ProPlus, version 7.0). Positive signals were quantified using the 'count-size' function and expressed as % positive area per thrombus area. TUNEL-positive apoptotic cells were detected on cross sections through the uninjured IVC segment of End.p53-WT and End.p53-KO mice using the In Situ Cell Death Detection kit (Roche) and manually counted.

Confocal microscopy

Two days or three weeks post surgery animals were anesthetized and venous tissue was isolated, as above, and fixed in fresh 4% paraformaldehyde (Sigma-Aldrich), followed by incubation in 15% and 30% sucrose (Roth). Immunofluorescence staining was performed on 8 µm-thick cryo-sections embedded in Tissue-Tek O.C.T. (Sakura). Sections were post-fixed in acetone for 10 min at -20°C and permeabilized in 0.05% Triton X-100 (in PBS; Roth) for 10 min at 37°C. Sections were incubated with antibodies against CD31 (clone Mec13.3; Santa Cruz Biotechnology), p53 (abcam), heparanase-1 (abcam), early growth response gene-1 (Egr-1; clone EPR3863; abcam), tissue factor (TF; abcam) overnight at 4°C followed by incubation with fluorescein- (FITC) or Alexa Fluor546-conjugated secondary antibodies (Molecular Probes) for 30 min at RT. Cell nuclei were visualized using 4',6-diamidine-2-phenylindole (DAPI; Roth). Sections were mounted in fluorescence mounting medium (Dako) and photographed on a confocal microscope (Leica SP8) using LAS X software. As negative control, the first antibody was omitted (a representative example is shown in Supplemental Figure S2).

Tail bleeding time

At the age of 12 weeks, male mice were anesthetized with 2% isoflurane, placed on a heating pad and subjected to tail tip amputation (approx. 2 mm) using surgical scissors. Tails were immediately immersed in a 50-mL tube containing 45 mL prewarmed 0.9% NaCl solution and the time to the first and the last bleeding stop (for at least 30 seconds) recorded. At the end of the observation period of 10 min, mice were returned to their cages, and the optical density of the solution was determined at 560 nm to quantify the total blood loss.

Blood cell count and plasma factor Xa activity assay

Blood was obtained from anesthetized female mice by cardiac puncture into 3.8% sodium citrate. A 100 µL-aliquot was removed and the complete blood cell count determined using an automated hematology analyzer (Sysmex KX21N™; Sysmex). The remaining blood was centrifuged at 3,000 rpm for 10 min, the supernatant (plasma) removed and stored at -80°C pending analysis. Plasma factor Xa activity was measured using the Spectrozyme FXa chromogenic assay (Sekisui Diagnostics).

Cell culture studies

Human Umbilical Vein Endothelial Cells (HUVECs; PromoCell) were cultured on plates coated with 0.2% gelatin (Sigma-Aldrich) in Endothelial Cell Growth Medium (PromoCell). Cells were serially passaged until permanent growth arrest. The number of population doublings (PD) was determined using the formula: $PD = X + 3.322 (\log Y - \log I)$, where 'X' represents the initial population doubling level, 'Y' the number of cells at the end of the growth period and 'I' the initial number of cells seeded per plate, according to the American Tissue Culture Collection (ATCC).[10] Cells were analyzed between passage 5 and 13. Senescent cells were visualized using the Senescence Detection kit (Abcam).

Isolation of primary murine endothelial cells

To isolate primary mouse pulmonary endothelial cells (mPECs), lungs were excised and diced into 1 mm-sized pieces. The tissue was digested in 1.5 mg/mL collagenase A (in PBS; Worthington) at 37°C for 30 min with vigorous mixing every 10 min. Digested tissue was meshed through 70 µm Falcon® cell strainers (Corning) and neutralized with Dulbecco's Modified Eagles Medium (DMEM; Gibco) containing 20% fetal bovine serum (FBS; Gibco). After a brief centrifugation, the cell pellet was resuspended in 1X PBS containing 0.5% FBS and 2 mM ethylendiaminetetraacetic acid (EDTA). First, non-endothelial cells were depleted using CD45 followed by labeling of endothelial cells with CD31-conjugated magnetic MicroBeads and sorting using magnetic separation LS columns (Miltenyi Biotech) CD31-sorted cells were immediately lysed using RIPA buffer containing PMSF (Cell Signaling Technologies) and processed for further analysis using Western blot.

Western blot analysis

Cells were snap-frozen on liquid nitrogen and resuspended in RIPA lysis buffer. Equal amounts of protein (25 µg) were fractionated by SDS polyacrylamide gel electrophoresis and transferred to nitrocellulose membranes (Protran®, Whatman). Membranes were blocked in 5% nonfat dry milk in TBS (0.1% Tween-20) followed by overnight incubation with antibodies against human or mouse CD31 (Dianova), Egr-1 (abcam), heparanase (ProSpec), p16INK4A (clone EPR1473; abcam), p53 (Santa Cruz Biotechnologies), phospho-histone 2A.X (p-H2A.X; Ser139; Cell Signaling Technologies), phosphatase and tensin homolog (PTEN; Cell Signaling Technologies), plasminogen activator inhibitor-1 (PAI-1; abcam), tissue factor (TF; clone EPR8986; abcam) and transforming growth factor-β (TGFβ; Novus Biologicals). Protein bands were visualized using horseraddish peroxidase-conjugated secondary antibodies (GE Healthcare) followed by SuperSignal® West Pico

Chemiluminescent Substrate (Thermo Scientific). Protein bands were quantified by densitometry and normalized to GAPDH (HyTest Ltd).

Statistical analysis

Normal distribution was examined using the d'Agostino-Pearson omnibus normality test. Quantitative data are presented as mean ± standard error of the mean (SEM) or as median [25% - 75% interquartile range]. If two groups were compared, Student's t-test for unpaired means was used, if samples were normally distributed, or Mann-Whitney test, if not. If more than two groups were compared, One-way ANOVA followed by Bonferroni's or Kruskall-Wallis followed by Dunn's multiple comparisons test were used. Non-parametric variables were examined using Pearson's χ^2 test. All analyses were performed using GraphPad PRISM data analysis software (version 6.0; GraphPad Software).

References

(1) Gogiraju R, Xu X, Bochenek ML, Steinbrecher JH, Lehnart SE, Wenzel P, Kessel M, Zeisberg EM, Dobbelstein M, Schäfer K. Endothelial p53 deletion improves angiogenesis and prevents cardiac fibrosis and heart failure induced by pressure overload in mice. *J Am Heart Assoc* 2015;4(2). pii: e001770. doi: 10.1161/JAHA.115.001770.

(2) Marino S, Vooijs M, van Der GH, Jonkers J, Berns A. Induction of medulloblastomas in p53-null mutant mice by somatic inactivation of Rb in the external granular layer cells of the cerebellum. *Genes Dev* 2000;14:994-1004.

(3) Forde A, Constien R, Grone HJ, Hammerling G, Arnold B. Temporal Cre-mediated recombination exclusively in endothelial cells using Tie2 regulatory elements. *Genesis* 2002;33:191-197.

(4) Hubert A, Bochenek ML, Schütz E, Gogiraju R, Münzel T, Schäfer K. Selective Deletion of Leptin Signaling in Endothelial Cells Enhances Neointima Formation and Phenocopies

the Vascular Effects of Diet-Induced Obesity in Mice. *Arterioscler Thromb Vasc Biol* 2017;37:1683-1697.

(5) Jäger M, Hubert A, Gogiraju R, Bochenek ML, Münzel T, Schäfer K. Inducible Knockdown of Endothelial Protein Tyrosine Phosphatase-1B Promotes Neointima Formation in Obese Mice by Enhancing Endothelial Senescence. *Antioxid Redox Signal* 2018. doi: 10.1089/ars.2017.7169. [Epub ahead of print]

(6) Brandt M, Schönfelder T, Schwenk M, Becker C, Jäckel S, Reinhardt C, Stark K, Massberg S, Münzel T, von Brühl ML, Wenzel P. Deep vein thrombus formation induced by flow reduction in mice is determined by venous side branches. *Clin Hemorheol Microcirc* 2014;56:145-152.

(7) von Brühl ML, Stark K, Steinhart A, Chandraratne S, Konrad I, Lorenz M, Khandoga A, Tirniceriu A, Coletti R, Kollnberger M, Byrne RA, Laitinen I, Walch A, Brill A, Pfeiler S, Manukyan D, Braun S, Lange P, Riegger J, Ware J, Eckart A, Haidari S, Rudelius M, Schulz C, Echtler K, Brinkmann V, Schwaiger M, Preissner KT, Wagner DD, Mackman N, Engelmann B, Massberg S. Monocytes, neutrophils, and platelets cooperate to initiate and propagate venous thrombosis in mice in vivo. *J Exp Med* 2012;209:819-835.

(8) Bonderman D, Jakowitsch J, Redwan B, Bergmeister H, Renner MK, Panzenbock H, Adlbrecht C, Georgopoulos A, Klepetko W, Kneussl M, Lang IM. Role for staphylococci in misguided thrombus resolution of chronic thromboembolic pulmonary hypertension. *Arterioscler Thromb Vasc Biol* 2008;28:678-684.

(9) Axelman E, Henig I, Crispel Y, Attias J, Li JP, Brenner B, Vlodavsky I, Nadir Y. Novel peptides that inhibit heparanase activation of the coagulation system. *Thromb Haemost* 2014;112:466-477.

(10) Hayflick L. The cell biology of aging. *Clin Geriatr Med* 1985;1:15-27.

Supplemental Table 1. Hematological parameter in adult and aged female End.p53-WT and End.p53-KO mice

	End.p53-WT mice	**End.p53-KO mice**	**End.p53-WT mice**	**End.p53-KO mice**	**P value**
age	adult	adult	aged	aged	
number	7	11	4	3	
leucocytes (x10³ per µL)	4.0 ± 0.2	3.9 ± 0.4	4.2 ± 0.6	2.7 ± 0.5	0.366
erythrocytes (x10^6 per µL)	6.0 ± 0.4	5.3 ± 0.4	5.7 ± 0.8	5.6 ± 0.6	0.547
platelets (x10³ per µL)	505 ± 85	498 ± 58	1077 ± 113 **	980 ± 129 *	0.0002
hemoglobin (g/dL)	9.7 ± 0.6	8.9 ± 0.6	8.0 ± 1.0	8.5 ± 0.8	0.290

Values are shown as mean ± SEM. *P<0.05 and **P<0.01 vs. adult mice of the same genotype (as determined by One-Way ANOVA followed by Bonferroni's multiple comparisons test). Similar findings were observed in male mice.

Supplemental Figure S1

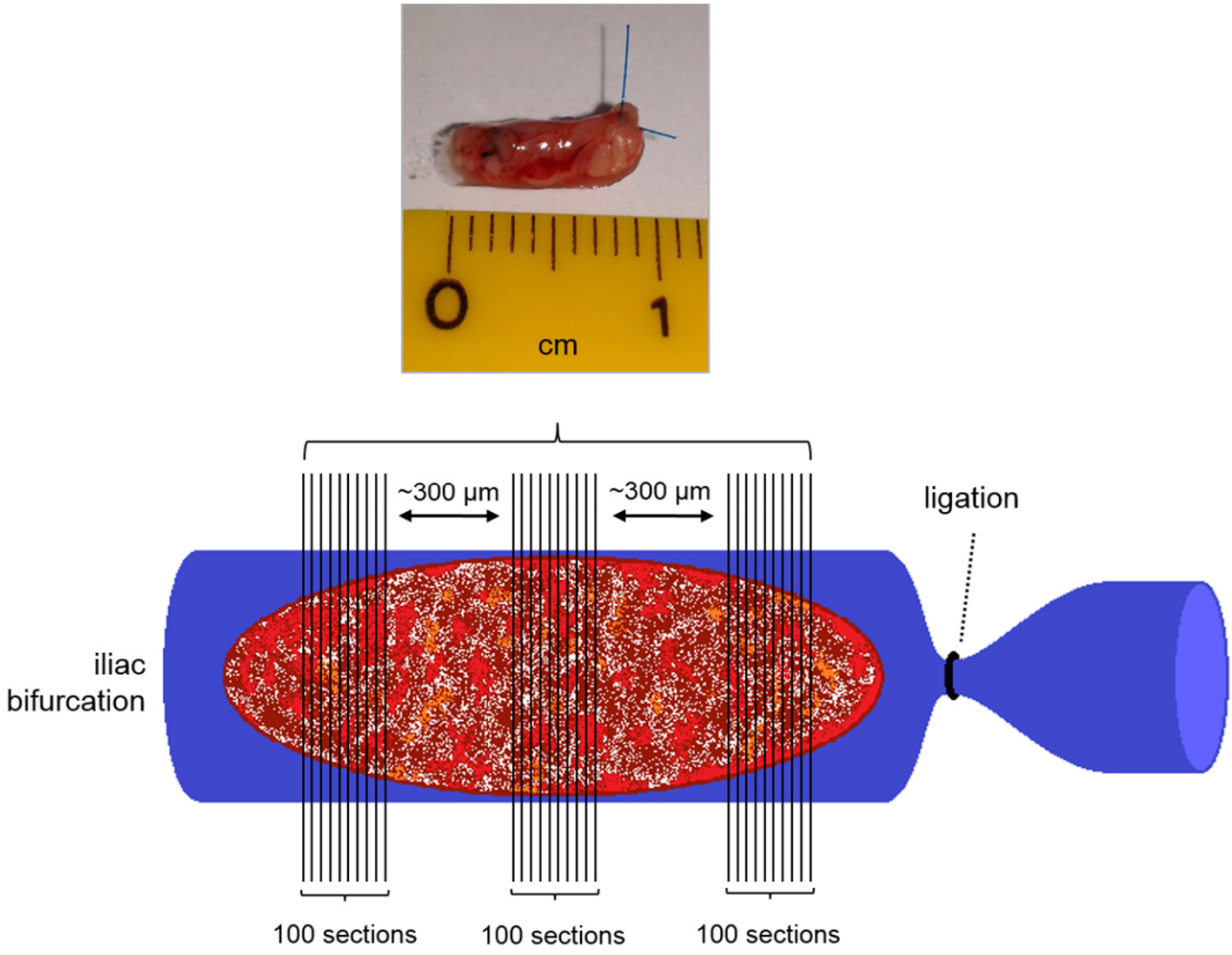

Supplemental Figure S1. Standardization of serial cross-section preparation through the *inferior V. cava*. Example of a ligated inferior V. cava (IVC) with thrombus (upper panel)) and schematic drawing demonstrating how sections through the thrombosed IVC of adult and aged End.p53-WT or End.p53-KO mice were prepared (lower panel): Five µm-thick cross-sections (4 per slide; 100 per series) were cut at 3 standardized intervals (approximately 300 µm apart) starting from immediately after the ligation towards the iliac bifurcation.

Supplemental Figure S2

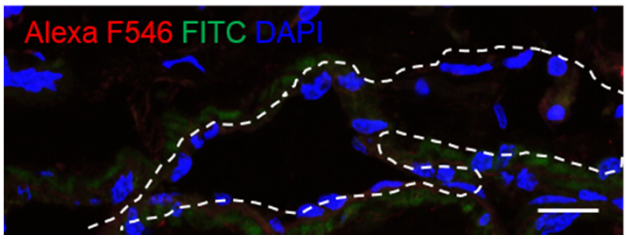

Supplemental Figure S2. Representative negative immunofluorescence control. Confocal microscopy image showing the results after staining of a cross-section through the uninjured inferior V. cava after omission of the primary antibody followed by incubation with Alexa Fluor 546- and fluorescein (FITC)-labeled secondary antibodies as well as DAPI to label cell nuclei. Broken white lines indicate the IVC lumen. Size bar represents 10 µm.

Supplemental Figure S3

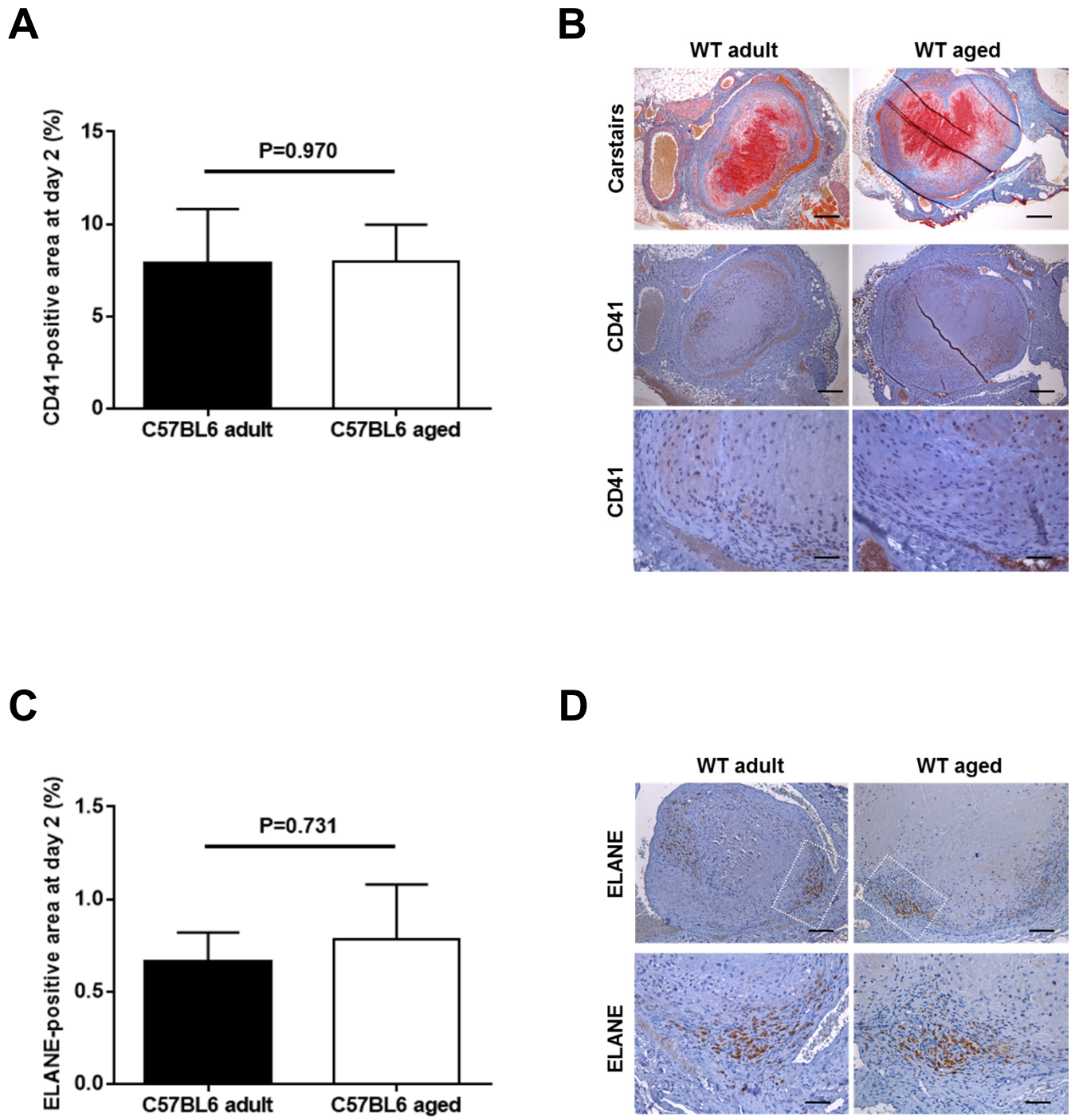

Supplemental Figure S3. Immunohistochemical analysis of platelets and neutrophils within 2 days-old venous thrombi. Thrombosed IVC segments of adult and aged C57BL6 mice (n=5 per group) were harvested at day 2 after surgery and examined for the presence of platelets or neutrophils using antibodies against CD41 (A and B) or neutrophil elastase (ELANE; C and D), respectively. Sections were also stained according to the Carstairs protocol to obtain a general overview of thrombus composition. (A) Quantitative analysis of the CD41-immunopositive area per thrombus area. (B) Representative images. Size bars represent 200 µm (top and middle row) and 100 µm (bottom row). (C) Quantitative analysis of the ELANE-immunopositive area per thrombus area. (D) Representative images. Size bars represent 100 (upper row) and 50 µm (bottom row). Individual values and the mean ± SEM are shown in (A) and (C). Statistical differences are indicated within the graphs.

Supplemental Figure S4

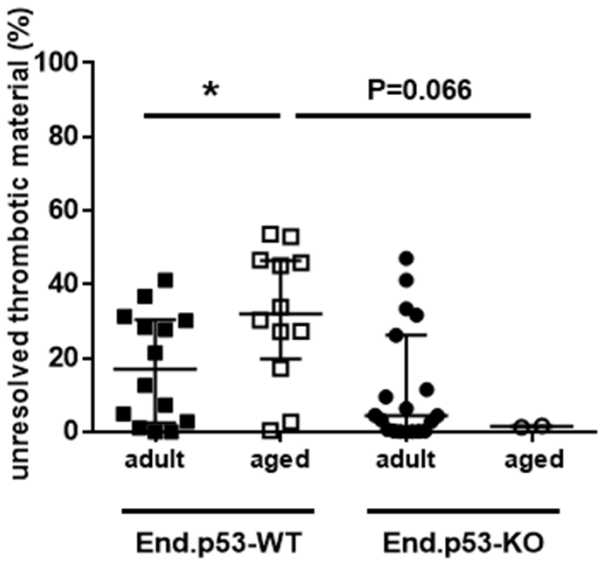

Supplemental Figure 4. Morphometric analysis of venous thrombi 3 weeks after IVC ligation. Serial cross sections through the thrombosed IVC segment of adult and aged End.p53-WT or End.p53-KO mice were examined 21 days after surgery and the relative amount of unresolved thrombotic material (red signal after Masson Trichrome stain) per total thrombus area quantified. Individual values and the median ± interquartile range are shown. *P<0.05. Representative images are shown in Figure 2F.

Supplemental Figure S5

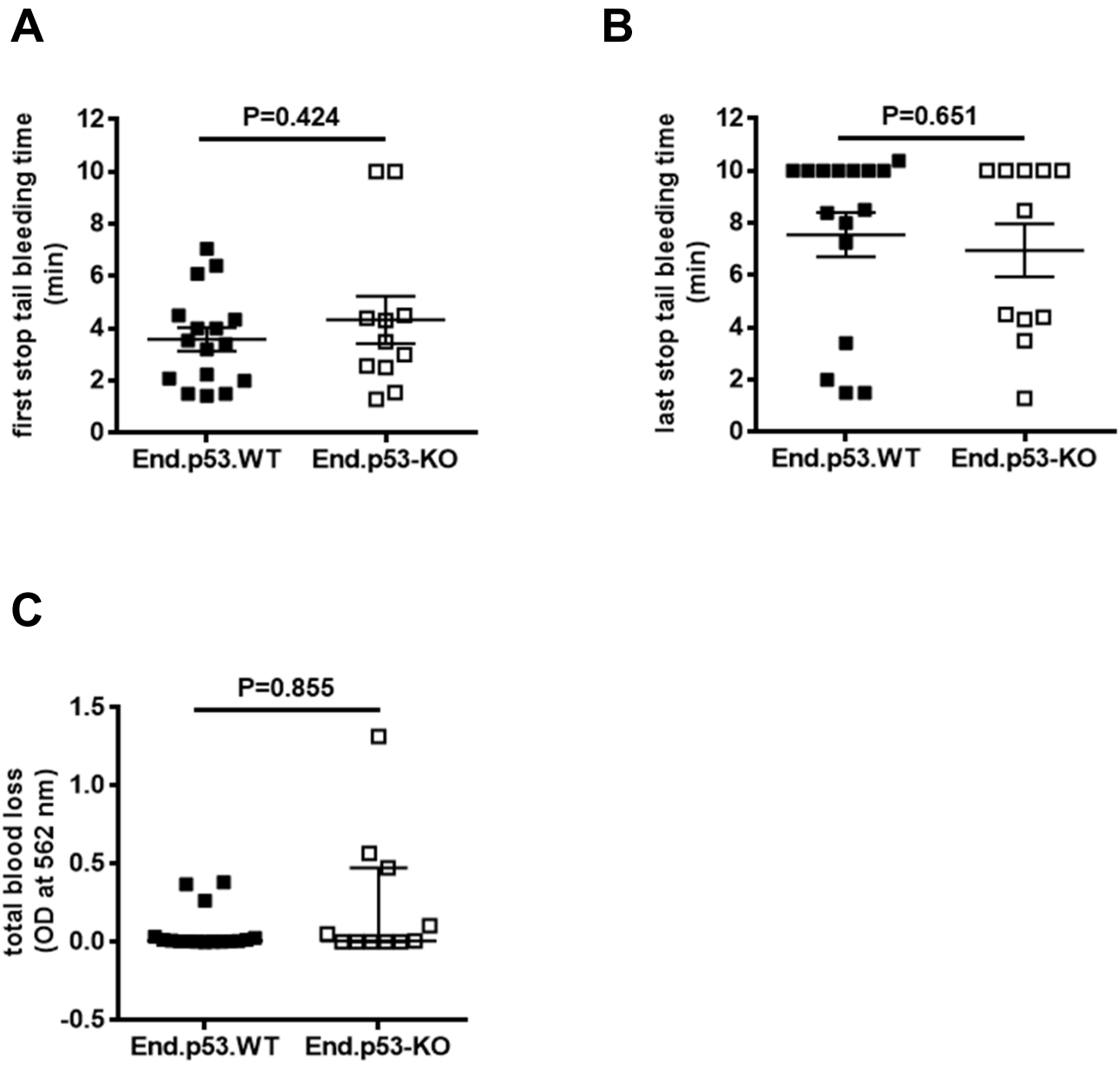

Supplemental Figure S5. Determination of tail bleeding time. Male End.p53-WT and End.p53-KO mice, aged 12 weeks, were examined for difference in their tail bleeding time. (A) Time to first bleeding stop and (B) time to last bleeding stop within the total observation time of 10 min. (C) Estimation of total blood loss determined spectrophotometrically at 562 nm. Graphs show individual values as well as the mean ± SEM (A and B) or median ± interquartile range (C) per group. Statistical differences are indicated within the graphs.

Supplemental Figure S6

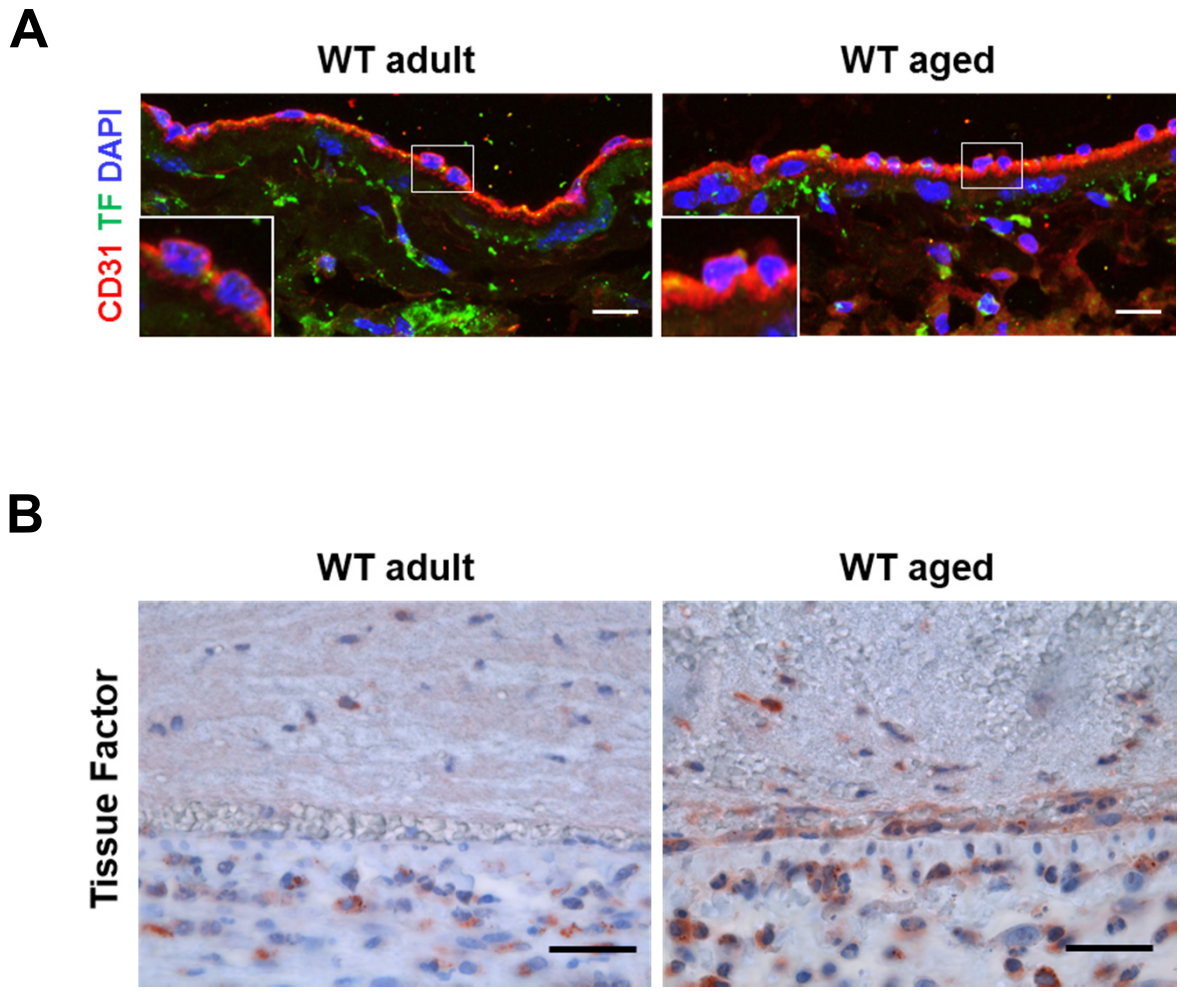

Supplemental Figure S6. Tissue factor expression in vein endothelium. (A) Cross-sections through the cryo-embedded uninjured *inferior V. cava* (IVC) of 12 weeks-old (adult) and 12 months-old (aged) wildtype (WT) mice were immunostained using antibodies against CD31 (red signal) or tissue factor (TF; green signal) and examined using confocal microscopy. DAPI was used to visualize cell nuclei (blue signal). Size bars represent 10 µm. (B) Paraffin-embedded cross-sections through the IVC at day 2 after ligation and induction of venous thrombosis were stained with antibodies against tissue factor followed by secondary antibodies and AEC reagent (red signal) and examined using light microscopy. Size bars represent 50 µm.

Supplemental Figure S7

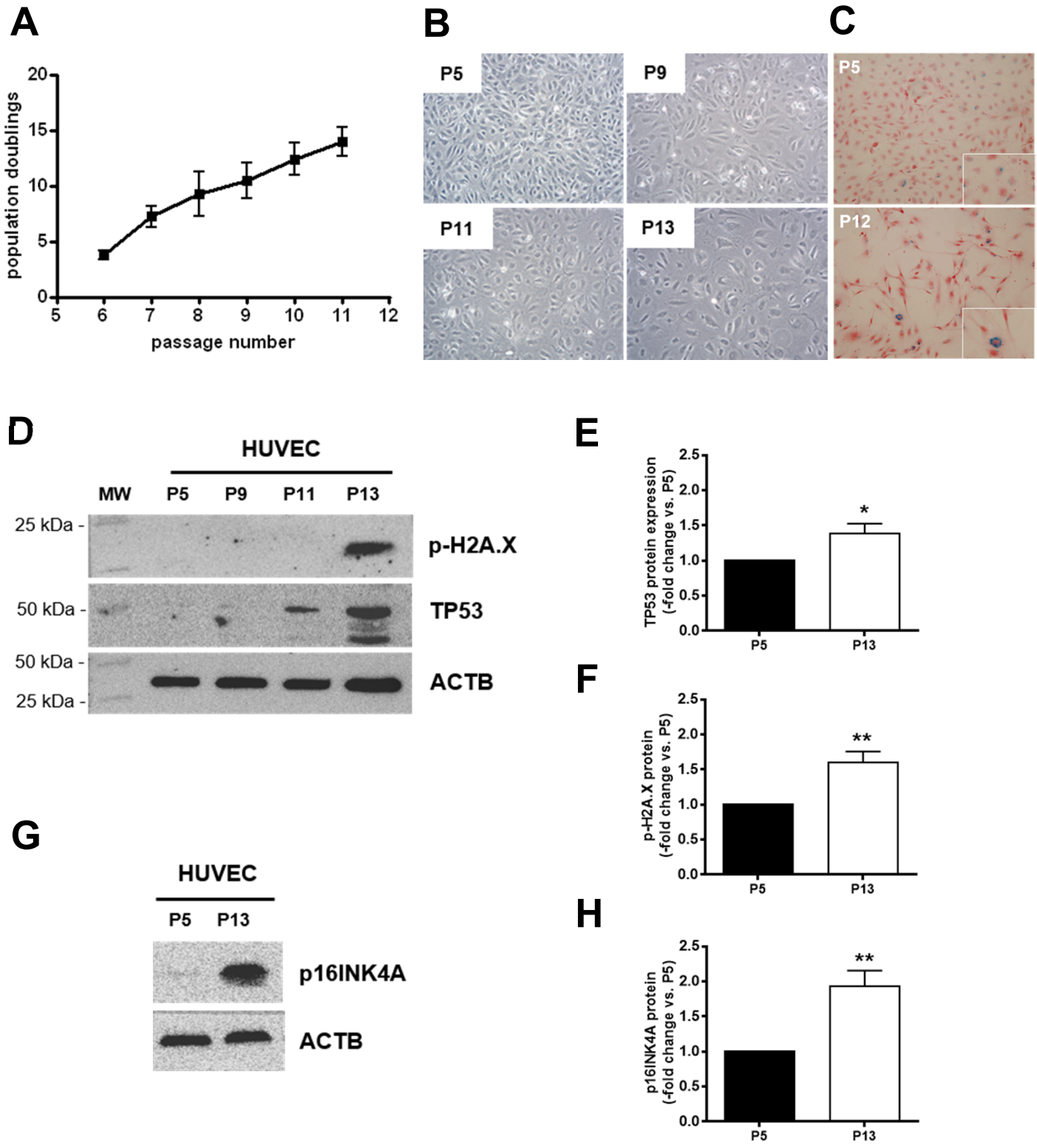

Supplemental Figure S7. Analysis of vascular senescence in human umbilical vein endothelial cells (HUVEC). (A) Calculated number of cumulative population doublings per passage number. (B) Representative phase contrast images of HUVECs at passage (P) 5, 9, 11 and 13. (C) Representative images of HUVECs at P5 and P12 after visualization of senescence-associated β-galactosidase activity (blue signal). Cell nuclei were counterstained using nuclear fast red. (D) Representative Western blot membrane showing expression of the senescence markers phospho-histone 2A.X (p-H2A.X) and tumor protein 53 (TP53; D) or p16INK4A (G). β-actin (ACTB) was used as control for equal protein loading. MW, molecular weight marker. Quantitative analysis of (E) p53, (F) p-H2A.X and (H) p16INK4A protein expression in HUVECs at P5 and P13. Summary of n=5 biological replicates. *P<0.05 and **P<0.01 vs. cells at P5.

Supplemental Figure S8

A

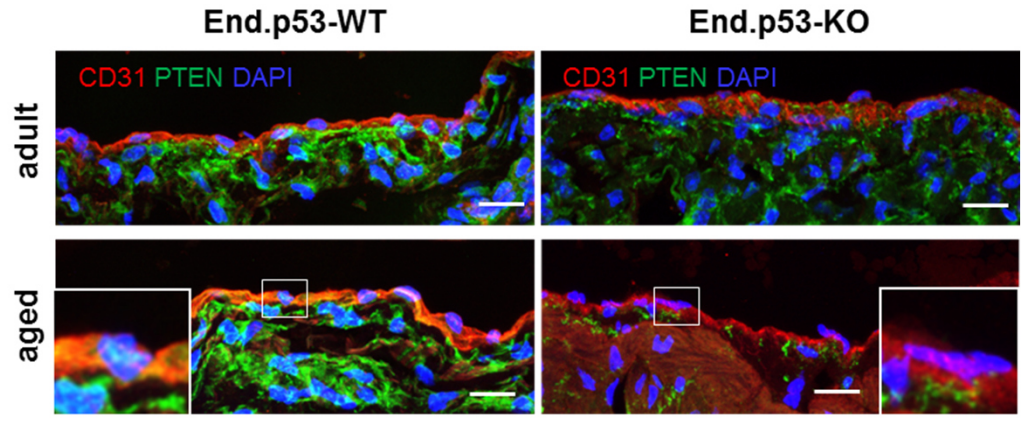

B

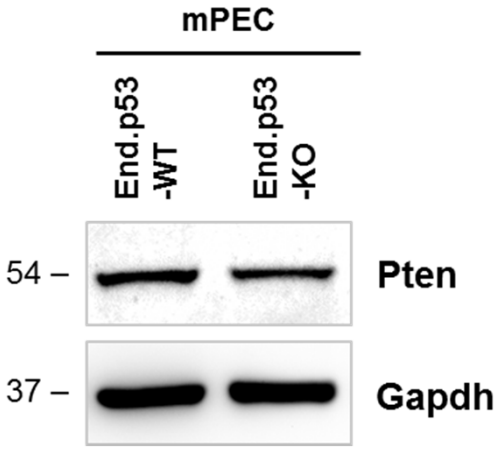

Supplemental Figure S8. Effect of genetic p53 deletion on endothelial p53 expression. (A) Confocal microscopy images after immunofluorescence detection of PTEN in uninjured inferior V. cava segments of adult and aged End.p53-WT and End.p53-KO mice. Endothelial cells were visualized using CD31 as marker, cell nuclei using DAPI. Size bars represent 10 µm. (B) Representative Western blot membrane showing the expression of PTEN in primary endothelial cells isolated from lungs (n=3 mice per isolation and genotype) of End.p53-WT and End.p53-KO mice. GAPDH is shown as control for equal protein loading.